A Study on to understand Diluted Magnetic Semiconductors

Kanu[1], Dr. Anil Kumar[2]

[1]Research Scholar, Sunrise University, Alwar, Rajasthan
[2]Research Supervisor, Sunrise University, Alwar, Rajasthan

Abstract

The utilization of both the charge and spin of electrons in electrical devices is known as "spin electronics," and DMSs play a crucial role in this field. Focusing on atomistic spin computations, this research examines how the geometrical characteristics of semiconductors affect their structural and magnetic properties. Stability is not seen because of the vast size of the system when it is reduced to a few nanometers. Using the Monte Carlo technique and the Heisenberg Hamiltonian VAMPIRE program, we theoretically investigate the magnetic characteristics of CoZnO materials in terms of size and shape effects. We find that magnetic disorder and temperature-dependent magnetization in Co-doped ZnO are governed by the material's size and shape. The research focuses on dilute magnetic semiconductors (DMS) such as $Ga_{1-x}Mn_xAs$ These are important components of semiconductor spintronics. They may be utilized as spin injectors and magnetic sensors thanks to their ferromagnetic characteristics. Therefore, we place emphasis on learning about the magnetic characteristics and establishing a solid method for calculating Curie temps from scratch. By bringing together first-principles calculations with statistical approaches like Monte Carlo simulations, we have built a theoretical framework for determining critical temperatures.

Keywords: RKKY, dilute magnetic semiconductor, Monte Carlo, size effect, shape effect.

1. INTRODUCTION

Using electrodes fabricated from alloys of ferromagnetic 3d metals, the initial generation of spintronics devices relied on passive magneto resistive sensors and memory components. Later, the discovery of enormous magnetoresistance in (Fe/Cr) n multilayers and tunneling magnetoresistance pushed their advancement forward. Devices of the next generation are projected to be active spin-based, which will need the synthesis and control of spin-polarized electrons in a host semiconductor. The electrons' spin polarization must be maintained to a great extent as they go through the semiconductor material for the device to function. Spin injection from an FM metal in a metal/SC connection is the most straightforward method.

Many researchers have tried to conserve electron spin across the interface of such heterostructures, but failed owing to the huge difference in electrical conductivity between the two materials. When it comes to signal amplification with highly spin-polarized carriers, however, magnetic semiconductors would be necessary and should provide simpler integration with the current semiconductor technology. Therefore, the development of such devices relies heavily on the design of materials integrating both SC and FM capabilities, which poses a significant problem in materials physics. The term "diluted magnetic semiconductor" (DMS) first appeared in this setting.

DMSs, which are non-magnetic semiconductors doped with a small number of magnetic materials, often transition-metals (TM), are anticipated to be not only highly spin-polarized but also readily integrable with existing semiconductors. However, it is turning out to be rather a formidable task in the field of solid-state research to find and comprehend such materials. Due to the need for both magnetic and electronic doping, as well as the need to design the interaction between magnetic dopant spins and free carriers to enable thermally durable dopant spin carrier coupling, developing suitable materials is a significant challenge. Some ferromagnetic semiconductors, such as europium chalcogenides and ferrimagnetic or ferromagnetic semiconducting spinels, are known to possess both magnetic and semiconducting characteristics.

However, all of this progress will inevitably halt when it becomes physically impossible to reduce the sizes any more. The field of spintronics enters at this point. The general concept is to build tools that take advantage of quantum physics rather than fight against it. Electrons have both electrical charge and spin, a wholly

(relativistic) quantum phenomena that cannot be described by conventional physics. Schematically, a spintronic device is one in which the spin is handled as opposed to the charge.

Figure 1. Schematic overview of spintronics which combines both charge (electronics) and spin (magnetism) into a novel field of research and applications.

The massive magneto resistance (GMR) read head in hard drives is unquestionably the most effective use of spintronics to date; this phenomenon was discovered by P. Grunberg and A. Fert, who shared the 2007 Nobel Prize in Physics for their work. The effect occurs, in the simplest of terms, when the electrical resistivity of a multilayer made of different magnetic and nonmagnetic materials depends on the magnetic configuration of the magnetic layers. Thin magnetic semiconductors, such as $Ga_{1-x}Mn_xAs$ materials that are highly sought after in the spintronics field. As little as a few percent of Mn impurities are all that's required to induce ferromagnetism. In this way, all-semiconductor spintronics may be accomplished by simply replacing the metallic ferromagnets. In addition, they are half-metallic and show a full spin polarization at the Fermi level E_F, making them excellent candidates for spin-dependent devices. The fact that the claimed Curie temperatures are so much lower than ambient temperature is easily their greatest drawback. Following, we will give some ab initio calculation results demonstrating the intricacy of these systems.

2. LITERATURE AND REVIEW

Akanksha Gupta et al (2020) Metal oxide semiconductor nanostructures with unusual magnetic characteristics have been the focus of intensive research and development over the last several years. Potential options with enhanced command over charge and spin degrees of freedom include dilute magnetic semiconductor oxides (DMSOs). Transparent DMSOs have a large band gap and exhibit induced ferromagnetism due to the presence of a small amount of magnetic 3d cation, which also results in a long-range antiferromagnetic order. Significant work has been done, however creating DMSO with ferromagnetic characteristics above room temperature remains a formidable obstacle. But large band gap materials like TiO_2, SnO_2, ZnO, and In_2O_3 (with 3.2 eV, 3.6 eV, 3.2 eV, and 2.92 eV, respectively) may host a wide variety of dopants to create new chemical structures. It is interesting to note that the grain boundary, existence of defects, and oxygen vacancies in these binary oxides, together with a decrease in size, may produce ferromagnetism even at room temperature. This article gives an overview of the structural analysis and magnetic characteristics of DMSOs based on binary metal oxides nanomaterials with different ferromagnetic or paramagnetic dopants, such as Co, V, Fe, and Ni, that have increased ferromagnetic behaviors at ambient temperature.

HikariShinya et al (2022) The potential benefits of dilute magnetic semiconductors (DMSs) for semiconductor spintronics applications have drawn increasing interest in this field. While much is known about Mn-doped III-V semiconductors, very little is known about other systems because of the lack of study in this area. Therefore, a thorough search for zincblende-type DMSs was done using the Korringa-Kohn-Rostoker Green function approach in conjunction with the coherent potential approximation (KKR-CPA), and it was discovered that (Al,Cr)P and (Al,Cr)As preserved ferromagnetism at high temperatures. Since the Curie temperature is overestimated by the mean-field approximation due to the neglect of the magnetic percolation effect, a Monte Carlo simulation was run to reproduce the experimental annealing procedure and estimate the Curie temperature using the random phase approximation, which takes into account the magnetic percolation effect. It has been

discovered that during annealing, the Cr atoms in the AlP and AlAs host semiconductors cluster together due to attractive interactions, forming nanoclusters. In addition, research into the effects of annealing conditions on the Curie temperature revealed that the annealing temperature may adjust the Curie temperature by changing the density and size of the Cr nanoclusters. In addition, it was concluded that the nanoclusters' forms may be modified by adjusting the parameters of crystal development. These findings are critical for facilitating material production for next-generation semiconductor spintronics.

Arif Babanlı et al (2022) Interband transitions are studied for their role in modifying the optical characteristics of a diluted magnetic semiconductor cylinder quantum dot. We investigate the effects of changing the quantum dot's operating conditions (temperature, magnetic field, and structural factors) on its response to a photon of varying energy. It is shown that the maximum of the absorption coefficient is sensitive to variations in the energy gap between electrons and holes in similar quantum states. The findings showed that when the temperature rose, the absorption maximum moved down to a lower energy level. The absorption maximum moves upward in energy as the magnetic field strength diminishes. It was also discovered that the absorption threshold frequency changes in a linear fashion at high temperatures and a nonlinear fashion at low temperatures as a function of the magnetic field.

Yu M Kuznetsov et al (2022) An alternative route to creating diluted magnetic semiconductors from gallium arsenide doped with iron and manganese atoms is discussed. Diffusion doping is performed in real time during pulsed laser deposition in a vacuum. In this case, X-ray photoelectron spectroscopy was used to get the profile of the distribution of chemical elements. The effect of magnetic phases on the behavior of the Hall resistance as a function of magnetic field is investigated. For the structure to develop with ferromagnetic characteristics at room temperature, certain technical criteria had to be settled upon.

Anielle C.A. Silva, et al (2021) Doping the semiconductor with transition metals (TM) creates a novel class of materials known as diluted magnetic semiconductors (DMS) nanocrystals, which exhibit intriguing magneto-optical features. Exchange interaction between sp-electrons in a pure semiconductor and localized TM d-electrons is responsible for these characteristics. Exciting novel DMS, in powder form and embedded in glassy systems, was produced by the group, and their findings are presented in this book chapter. Saturation of the inclusion of substitutional and interstitial sites in the nanocrystal structure, leading to the formation of additional nanocrystals, may occur at a certain concentration of doping ions. Doping saturation limit studies were conducted on DMS $Zn_{1-x}Mn_xO$ NCs, $Zn_{1-x}Mn_xTe$ NCs, $Zn_{0.99-x}Mn0.01CoxTe$ NCs, and $Bi_{2-x}Co_xS$ NCs produced in glassy matrices. Saturation of the sites into the crystalline lattice of nanocrystals is therefore a subject seldom documented in the literature, and we will provide commentary on this study. Thus, in this paper, we will demonstrate the group's findings about modulation and saturation in diluted magnetic semiconductor nanocrystals.

3. METHODOLOGY

The magnetic properties of Co-doped ZnO are investigated over a range of dimensions and forms. The hexagonal wurtzite (WZ) type is the most common form of pure ZnO, and its tetrahedral nearest-neighbor atomic coordination is very close to that of the cubic zincblende (ZB) type. The WZ structure of ZnO, with lattice parameters a = b = 3, 262 A and c = 5, 226 A, is used in our computations. Here, we use an atomistic spin model with the Heisenberg form of exchange to predict the magnetic behavior of Co-doped ZnO. This model describes the interaction between two spins on nearby atomic sites.

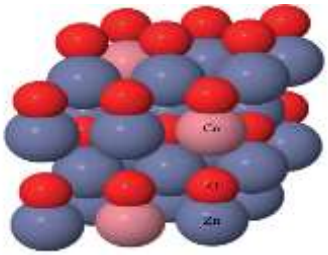

Figure 2. The crystal structure of the Zn 1−x Cox O wurtzite lattice. Here spheres represent Zn, O, and Co atoms.

The total energy of the system may be described by a classical Heisenberg model, but first the spin system must be uncoupled from the lattice and the electronic system. As a result, the following is the shape of the classical spin Hamiltonian we examine:

$$H = -\sum_{i \neq j} J_{ij} \vec{S}_i . \vec{S}_j - d_e \left(\vec{S}_i . e \right)^2 - |\mu_s| . \vec{H}_{app} . \vec{S}_i$$

where d_e represents the constant of uniaxial anisotropy, and H_{app} is the field that is applied from outside. Heisenberg's model includes the exchange interaction energy, the uniaxial energy component, and the Zeeman energy term in this case.

$\vec{S}_i$ and $\vec{S}_j$ are the quantum mechanical spins of the atomic sites. μ_s is the atomistic spin moment and J_{ij} is a necessary part of the trade. The Ruderman-Kittel-Kasuya-Yosida (RKKY) approach is often used to characterize the exchange interaction at low to medium concentrations, when spin-spin interactions are mediated by the conduction electrons. The following formula describes how we apply RKKY to the exchange interactions between the spins of the Co atoms:

$$J_{ij} = J_{RKKY} = -j_0 e^{r/l} \left[\frac{2k_F r.Cos\left(2k_F r\right) - Sin\left(2k_F r\right)}{\left(2k_F r\right)^4} \right]$$

Where $\mathbf{J_0 = 20 \times e^{-22}}$ In this equation, J represents the typical exchange energy in lightly and moderately doped transition metals, r represents the distance between the two nearest neighbor spins, l represents the damping scale of the RKKY interaction caused by the localization of the carriers, and l + 1 represents the average exchange energy $\mathbf{e^{r/l} \cong 10}$ Since electrons are unable to hop huge distances, the term restricted conductivity arises from the RKKY interaction's limited conductivity setting. As a result of translational equivalence, the exchange integral J_{ij} depends only on the distance $r_i - r_j$ between spins. For medium concentrations, $\mathbf{k_F \cong 10}$ is the vector of the Fermi wave, which relies exclusively on the number of electrons, or the Fermi momentum. Applying the VAMPIRE atomistic spin package software, which is based on the Monte Carlo approach, we predict the magnetic behavior of CoZnO from the classical spin Hamiltonian.

DMS like $Ga_{1-x}Mn_xAs$ are promising for use in a semiconductor-free spintronics. While significant advances and a large number of published publications have been made, the lack of commercially available DMS with a Curie temperature T_c above room temperature remains a major obstacle to widespread use. Consequently, one of the most pressing issues in spintronics is the development of methods for understanding, forecasting, and achieving DMS at temperatures higher than room temperature. The maximum T_c of DMS recorded is about 170 K for 8% Mn doped GaAs, which is too low for applications.

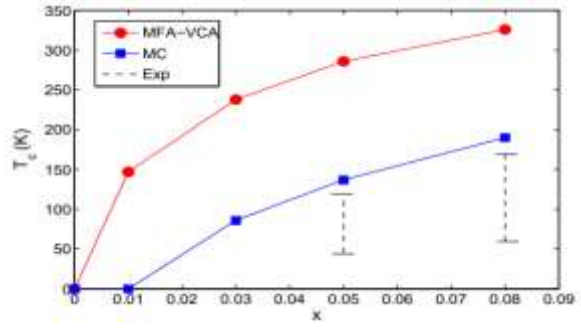

Figure 3. Calculated Curie temperatures of Mn-doped GaAs as a function of Mn concentration x using the mean field approximation (MFA-VCA) and Monte Carlo simulations (MC). The exchange coupling parameters are calculated from LDA.

Percolation and disorder effects have also been shown to significantly suppress ferromagnetism in these systems. An LDA-calculated Curie temperature for Mn-doped GaAs is shown below, plotted against the

concentration of Mn-atom substitutes. Percolation appears to provide a general hurdle for high T_c in DMS, since even the most precise approach, MC simulations, produces T_c values that are much lower than earlier mean field estimates (MFA-VCA). Since the interaction range is so small in DMS with a broad band gap, such as (Ga,Mn)N or (Zn,Cr)Te, they are especially well suited for applications where precision is required. Even though the interaction is rather long ranging in (Ga,Mn)As, this has a considerable impact.

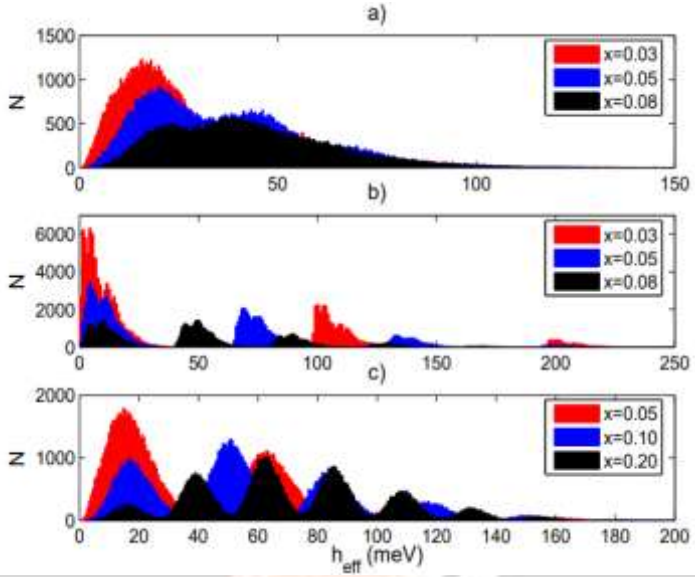

Figure 4. Distributions of local magnetic fields for a) Mn-doped GaAs, b) Mn-doped GaN and c) Cr-doped ZnTe. x denotes the concentration of magnetic impurities.

We have analyzed the local effective magnetic fields to better understand why the mean field approximation combined with the virtual approximation (MFA-VCA) sometimes fails totally, while at other times yields good results h^{eff} DMS-related items. In order to elaborate, the h^{eff} which means

$$h_i^{\text{eff}} = \sum_j J_{0j} \langle S_j^z \rangle,$$

for each magnetic site i and at $T = 0K, \langle S_j^z \rangle = 1$ Each location I in a non-random system always has the same value of h^{eff}. Instead, we will see a dispersion of local effective magnetic fields, like what is shown for Mn-doped GaAs, Mn-doped GaN, and Cr-doped ZnTe, in a random system like DMS, where each site has a unique local environment.

At greater concentrations, the distribution of Mn-doped GaAs is not drastically different from a Gaussian. Consequently, the DMS system where the MFA-VCA estimate is closest to the true MC value is the one we'll focus on in this article (approximately a factor of 2 too large). Everything is different in GaN. The distribution does not even remotely like a Gaussian; rather, it has several peaks (arising from the dominant interactions in the 110-direction). This distribution makes it obvious that the MFA-VCA estimate is extremely off, which turns out to be the case (the exact MC values are about one order of magnitude lower). With Cr-doped ZnTe, the distribution has many smaller peaks, making it an intermediate instance. However, the MFA-VCA estimate is somewhat better since the magnetic atom concentration is higher than in the previous two examples.

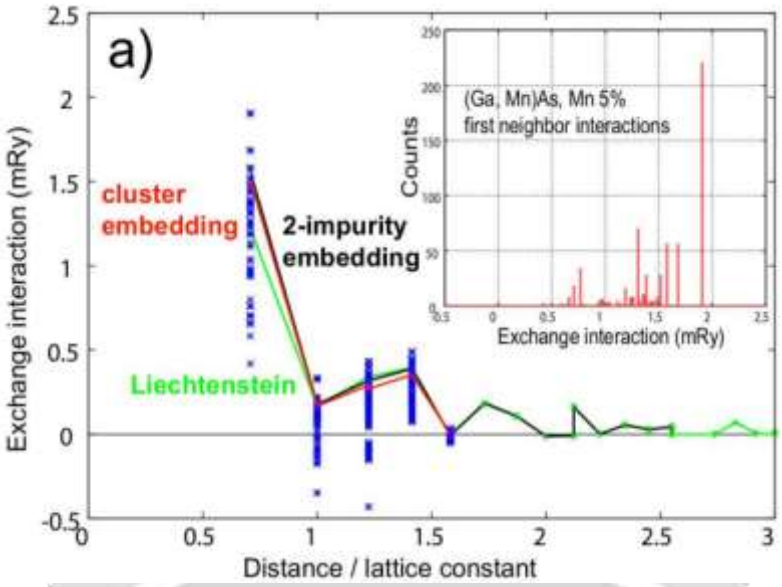

Figure 5. Exchange interactions in 5% Mn-doped GaAs using cluster embedding in CPA medium as a function of distance. The inset shows the distribution of nearest neighbour interaction.

We have calculated and analyzed his issue in great depth J_{ij} for an embedded CPA medium consisting of a sequence of locally disturbed environments (clusters). Large variations in the area observed in the data (Figure 5) J_{ij} information, which is very sensitive to the localization of third- and fourth-order Mn impurities at coordinates I and j. Nearest neighbor values and their frequency distribution are shown in the inset. J_{01}. At least for closest neighbor interactions, the configurational average does not match with the Lichtenstein-based CPA findings. Assuming the 2-impurity issue is solved properly, however, it fits well with the precise findings for two impurities I and j embedded in the CPA medium, demonstrating that the disorder is well characterized by the CPA.

4. RESULTS

Given the above, we use a classical Heisenberg spin model with RKKY exchange interactions between Co ions to mimic the magnetic characteristics of Co-doped ZnO. This research included the magnetic calculations of $Zn_{1-x}Co_xO$ depend on the amount of Co, and the results are analyzed using the VAMPIRE software. In this setup, we utilize a supercell with cell dimensions of 555 and 151515, and we apply periodic boundary constraints. The effects of Co doping are investigated when we randomly inject the element into ZnO crystals of various sizes and shapes. The magnetic characteristics of Co (30%)-doped ZnO are simulated by field cooling magnetization, which is typically measured in a weak magnetic field. We make an approximation of the inter spin interaction strengths. behavior inconsistent with full ferromagnetism with an applied field of 1 T. The system's size is reduced to a few nanometers, and stability is not seen, depending on the size, shape, and temperature. We also model the size and shape-dependent magnetic behavior of materials. The change from ferromagnetic to paramagnetic is well delineated. size-dependent paramagnetic and weak ferromagnetic characteristics. in contrast, has distinct weak ferromagnetic activity for each of its three possible crystal forms (cube, cylinder, and sphere).

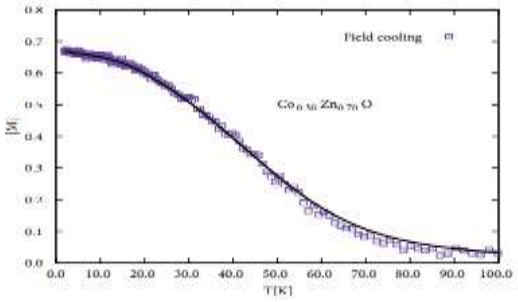

Figure 6. Field cooled magnetization curve for the $Co_{0.3}Zn_{0.7}O$ diluted magnetic semiconductor. Observed curves are obtained for the long-range ferromagnetism in the presence of ferromagnetic correlations. The system is cooled from 100 K to 0 K by 10,000 Monte Carlo steps.

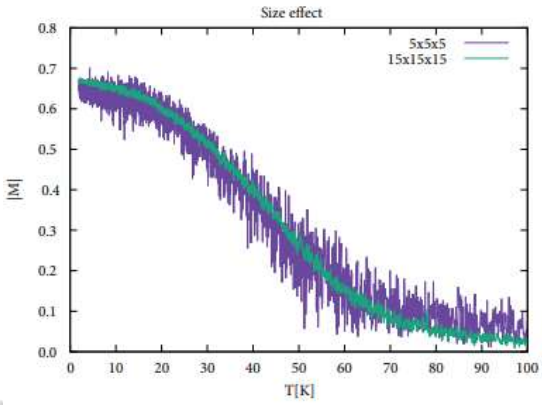

Figure 7. Temperature dependence of magnetism for different system sizes. These curves show magnetic disorder at different sizes. As the size of the system increases, the magnetic defects disappear. Temperature-dependent magnetization measurements were performed at fixed field and uniaxial anisotropy values.

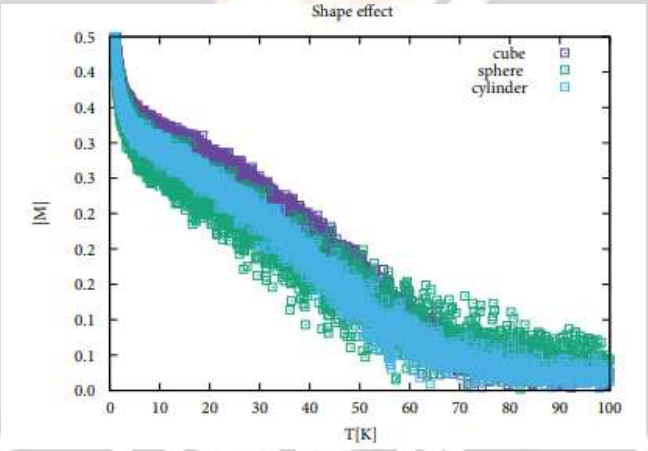

Figure 8. Different crystal structures and magnetic behaviors: cube, cylinder, and sphere. These tendencies of magnetic disorder are due to the existence of a variety of magnetic ground states commonly associated with spin-glass behaviors. The magnetic behavior of CoZnO nanoparticles was measured at various shapes from 0 K to 100 K.

5. CONCLUSION

This study set out to learn how the dimensions and shape of Co-doped ZnO nanoparticles affect their magnetic properties. Using a Heisenberg exchange coupling model, we have explained the magnetic behavior of DMSs in the medium density domain. The RKKY approach, which is appropriate for describing the exchange coupling process, has been used to calculate the magnetic exchange coupling constant as a function of Co concentration in ZnO materials. Understanding the magnetic characteristics of DMSs and seeing the phase behavior by adding diluted systems are significant outcomes of the current theory. The size and form impact on 30% Co-doped ZnO have been investigated by manipulating several material factors including temperature and applied external field. Nanoparticles and their oxides could have significant ferromagnetism effects due to their tiny size. The strength of the ferromagnetic effect grows in proportion to the size of magnetic nanoparticles. For these particles to be further developed, particularly for optoelectronic applications, we believe that size and shape impacts and doping ratio will play crucial roles. We have provided a theoretical examination of diluted magnetic semiconductors, a promising material for potential future applications in spintronics, utilizing a mix of quantum

mechanical computations and statistical approaches. The critical temperatures are, however, still too low for any real-world applications.

6. REFERENCES:

1. Gupta, Akanksha & Zhang, Rui & Kumar, Pramod & Kumar, Vinod & Kumar, Anup. (2020). Nano-Structured Dilute Magnetic Semiconductors for Efficient Spintronics at Room Temperature. Magnetochemistry. 6. 15. 10.3390/magnetochemistry6010015.
2. Hikari Shinya, Takaya Kubota, Yuichiro Tanaka, Masafumi Shirai, Design of novel dilute magnetic semiconductors by exhaustive first-principles calculations and scale-bridging simulations, Materials Today Communications, Volume 31, 2022, 103604, ISSN 2352-4928, https://doi.org/10.1016/j.mtcomm.2022.103604.
3. Babanlı, Arif & Sabyrov, Vepa. (2022). Optical properties of cylindrical quantum dots with diluted magnetic semiconductor's structure. Low Temperature Physics. 48. 825-831. 10.1063/10.0014026.
4. Yu M Kuznetsov, M V Dorokhin, R N Kryukov , A V Zdoroveyshchev, D A Zdoroveyshchev and V P Lesnikov (2022) Formation of the diluted magnetic semiconductor phase by thermal diffusion in the pulsed laser deposition method RYCPS-2021 Journal of Physics: Conference Series 2227 (2022) 012003 IOP Publishing doi:10.1088/1742-6596/2227/1/012003
5. Silva, Anielle et al. "Diluted Magnetic Semiconductors Nanocrystals: Saturation and Modulation". Materials at the Nanoscale, edited by Awadesh Mallik, IntechOpen, 2021. 10.5772/intechopen.96679.
6. Mancer, Hemza & RACHED, Habib. (2022). First-Principles Study Of Electronic Structure And Magnetic Properties Of Diluted Magnetic Semiconductor Be1-xFexS.
7. Lourenço, S.A.; Dantas, N.O.; Souza, R. On Synthesis, Optical and magnetic Properties of Semi magnetic Nanocrystals Growth in Glass Matrix. Nano magnetism 2014, 53-73.
8. Silva, R.S. da; Neto, E.S. de F.; Dantas, N.O. Optical, Magnetic, and Structural Properties of Semiconductor and Semi magnetic Nanocrystals. In Nanocrystals - Synthesis, Characterization and Applications; 2012.
9. Schulz, H.J. Transition metal impurities in compound semiconductors: Experimental situation - ScienceDirect. Mater. Chem. Phys. 1987, 16, 373-384.
10. Oliveira, N.; Freitas Neto, E.S. De; Da Silv, R.S. Diluted Magnetic Semiconductor Nanocrystals in Glass Matrix. In Nanocrystals; 2010.
11. Cibert, J.; Scalbert, D. Diluted Magnetic Semiconductors: Basic Physics and Optical Properties. In; Springer, Berlin, Heidelberg, 2008; pp. 389-431.
12. Wang, C.; Yang, F.; Gao, Y. The highly-efficient light-emitting diodes based on transition metal dichalcogenides: From architecture to performance. Nanoscale Adv. 2020, 2, 4323-4340.
13. Rai, D.P.; Laref, A.; Shankar, A.; Sandeep; Sakhya, A.P.; Khenata, R.; Thapa, R.K. Spin-induced transition metal (TM) doped SnO2 a dilute magnetic semiconductor (DMS): A first principles study. J. Phys. Chem. Solids 2018, 120, 104-108, doi: 10.1016/j.jpcs.2018.04.006.
14. Morandi, O.; Hervieux, P.A.; Manfredi, G. Laser induced ultrafast demagnetization in diluted magnetic semiconductor nanostructures. In Proceedings of the European Physical Journal D; 2009; Vol. 52, pp. 155-158.
15. Brozek, C.K.; Zhou, D.; Liu, H.; Li, X.; Kittilstved, K.R.; Gamelin, D.R. Soluble Supercapacitors: Large and Reversible Charge Storage in Colloidal Iron-Doped ZnO Nanocrystals. Nano Lett. 2018, 18, 3297-3302, doi: 10.1021/acs.nanolett.8b01264.